Supporting Information

Palladium modified cuprous (I) oxide with {100} facets for photocatalytic CO_2 reduction

Xiaojing Zhang [a], Xin Zhao [b,c], Ke Chen [a], Yingying Fan [a□], Shilei Wei [a], Wensheng Zhang [a], Dongxue Han [a,c□] and Li Niu [a,c]

[a] *School of Civil Engineering c/o Center for Advanced Analytical Science, School of Chemistry and Chemical Engineering, Guangzhou University, Guangzhou 510006, P. R. China. E-mail: dxhan@gzhu.edu.cn; ccyyfan@gzhu.edu.cn*

[b] *State Key Laboratory of Electroanalytical Chemistry, c/o Engineering Laboratory for Modern Analytical Techniques, CAS Center for Excellence in Nanoscience, Changchun Institute of Applied Chemistry, Changchun 130022, P. R. China*

Work function calculation

$$\Phi = E_{vac} - E_F \quad (1)$$

$$\chi = E_{vac} - E_{CB} \quad (2)$$

$$E_g = E_{CB} - E_{VB} \quad (3)$$

The calculations of work function about Cu_2O were taken by the above equations [1]. Where χ is the semiconductor electron affinity, E_{CB} is the conduction band maximum edge potentials, E_{VB} is the valence band maximum edge potentials, E_F is the Fermi level, and E_g is the band gap. The value of the semiconductor electron affinity is 3.20 eV for $111Cu_2O$ and 3.56 eV in $100Cu_2O$ [2-4]. E_g is obtained as 1.90 eV for $100Cu_2O$ and 1.91 eV for $111Cu_2O$ by the measurements of UV-Vis DRS (Fig. 3a). According to the valence band spectra (Fig. 3b), the energy gap between E_f and E_{VB} is estimated individually at about 0.23 and 0.12 eV for $100Cu_2O$ and $111Cu_2O$. Thus, based on the equation (1), (2) and (3), corresponding work function of $100Cu_2O$ and $111Cu_2O$ is achieved as 5.23 and 4.99 eV, respectively.

Q.E. calculation

In our experiment, QE is calculated based on *GB/T 26915-2011*. Taken 100Cu_2O as sample, during the photocatalytic reaction, the irradiation area (S) is 19.63 cm^2; the intensity of illumination (I) is 1.97 mW/cm^2; since the Xe lamp assembled with 420 nm filter was used in our work, the equivalent incident wavelength ($\bar{\lambda}$) can be considered as 584.30 nm (*GB/T 26915-2011*). Therefore, the incident photon is calculated to be 4.10×10^{20} quanta using the following equation:

$N_p = (I \times S \times t) / (hc / \bar{\lambda}) = (1.97 \times 10^{-3} \times 19.63 \times 3600 \times 584.3 \times 10^{-9}) / (6.62 \times 10^{-34} \times 3 \times 10^{8}) = 4.10 \times 10^{20}$

Based on the previous report [5], The reduction of CO_2 to CO is a two-electron transformation:

$CO_2 + 2H^+ + 2e^- \rightarrow CO + H_2O$

In our work, the CO yield rate of 100Cu_2O is 0.04 umol/h/g (Fig. 5), thus QE of 100Cu_2O can be calculated using the following equation:

$QE = (N_{CO} \times 2) / N_p = (0.04 \times 10^{-6} \times 6.02 \times 10^{23} \times 2) / (4.10 \times 10^{20}) \approx 0.01\ \%$

Since negative pressure (-0.04 MPa) was applied in our work (Fig.S6), companying with a low initial carbon source concentration and limiting the accumulation of CO, this value is reasonable. Likewise, the QE of 100Cu_2O-Pd, 111Cu_2O, 111Cu_2O-Pd is calculated to be 0.04%, 0.01%, 0.01%, respectively, suggesting that the loading of Pd on 100Cu_2O can efficiently promote the photoreduction activity of CO_2.

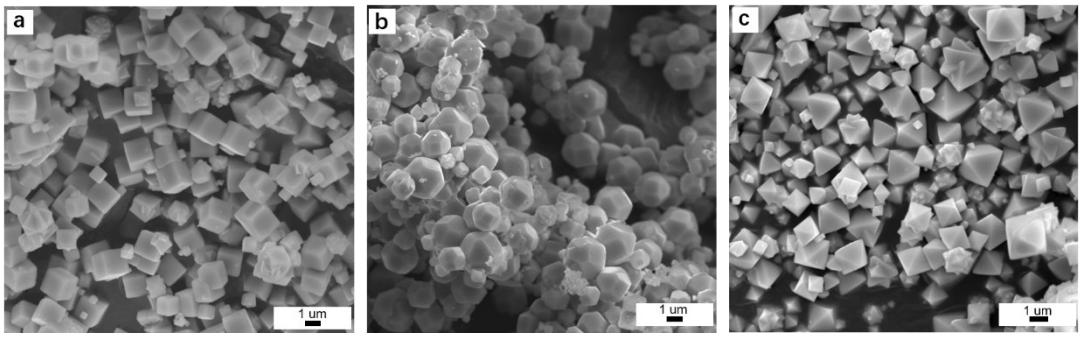

Fig. S1 SEM images of Cu_2O with different addition amounts of PVP (a) 0 g, (b) 0.2 g and (c) 1 g.

In the actual process, the influence of different PVP amounts on the synthesis of Cu_2O was explored. As shown in Fig. S1, cube Cu_2O was successfully prepared in the absence of PVP. When 0.2g PVP was used in the reaction, cubo-octahedron Cu_2O was obtained. Moreover, octahedron Cu_2O could be synthesized as the amount of PVP increases to 1.0 g.

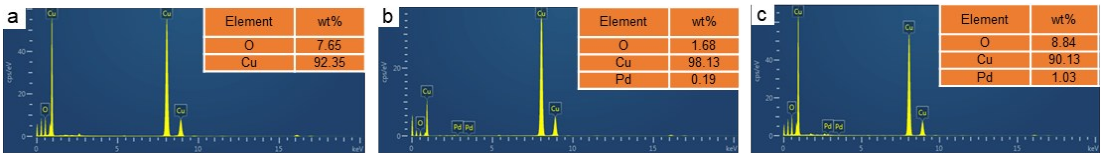

Fig. S2 EDX of (a) 111Cu_2O, (b) 111Cu_2O-0.03Pd and (c) 111Cu_2O-0.1Pd.

Energy dispersive X-ray (EDX) spectroscopy was used to explore the loading amount of Pd. As shown in Fig. S2, with the increase of additional K_2PdCl_4, the weight ratio of Pd raises from 0 (Fig. S2a), 0.18 (Fig. S2b) to 1.03 wt% (Fig. S2c) for 111Cu_2O (Fig. 1c), 111Cu_2O-0.03Pd (Fig. S4b) and 111Cu_2O-0.1Pd (Fig. 1f). The prominent promotion in mass ratio of Pd is consistent with the amount display in SEM images confirming that the loaded species on the surface of 100Cu_2O should be Pd nanoparticle.

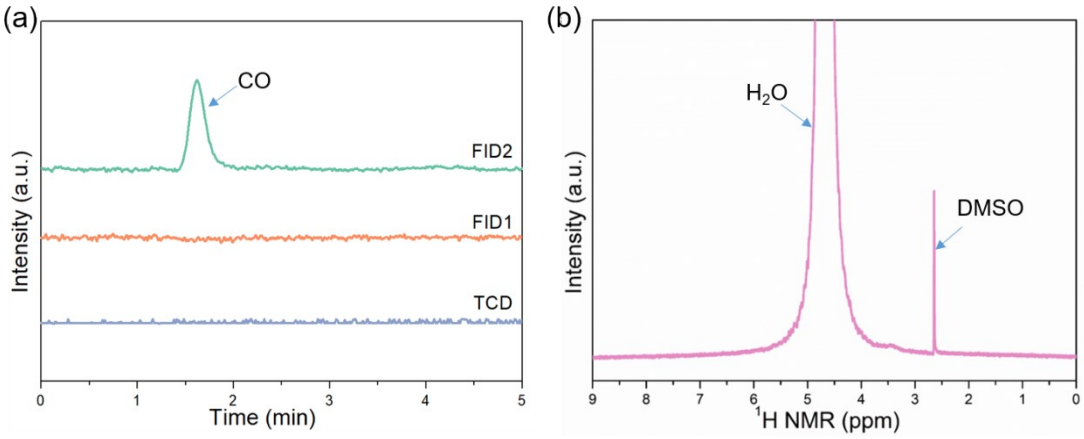

Fig. S3 (a) Gas chromatography and (b) ^{1}H NMR detection over 100Cu_2O-0.1Pd after 2h photoreduction of CO_2

The photocatalytic products of CO_2 reduction were detected by gas chromatography (GC) and nuclear magnetic resonance (NMR). H_2 as a possible gas product was evaluated by using the thermal conductivity detector (TCD) of GC equiped with packed column of 5A Φ 3 mm × 3 m. And other possible gas products including CO and CH_4 were estimated by the utilization of flame ionization detector (FID2) of GC assembled with packed column of GDN-502 Φ 3 mm × 4 m. The possible liquid products including formic acid, methanol and ethanol were assessed by the flame ionization detector (FID1) of gas chromatograph, which is equipped with capillary column of SE-54 Φ 0.32 mm × 50 m. The detection results were illustrated in Fig. S3a and there is only a peak of FID2 was observed, indicating there is absence of H_2, formic acid and methanol, ethanol. According to the standard substance, the observed peak in FID2 is ascribe to CO. ^{1}H NMR was also taken to further define the liquid product and recorded on Fig. S3b. Only two peaks which represented a signal of H_2O and internal standard (dimethyl sulfoxide, DMSO) were detected, indicating no CH_3OH (δ = 3.28 ppm) and HCOOH (δ = 8.30 ppm) as liquid products were generated. These results suggest that the discoverable product of CO_2 photoreduction over 100Cu_2O-Pd is only carbon monoxide.

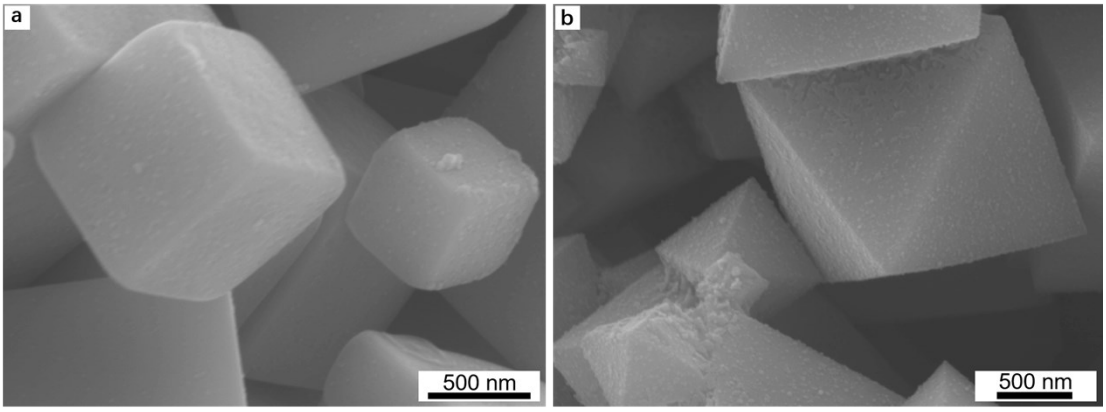

Fig. S4 SEM images of 100Cu_2O-0.30Pd and (b) 111Cu_2O-0.01Pd.

Fig. S4 shows the SEM images of Cu_2O covered with 3 wt% Pd, where 1 mL K_2PdCl_4 was uesed in this synthesis process.

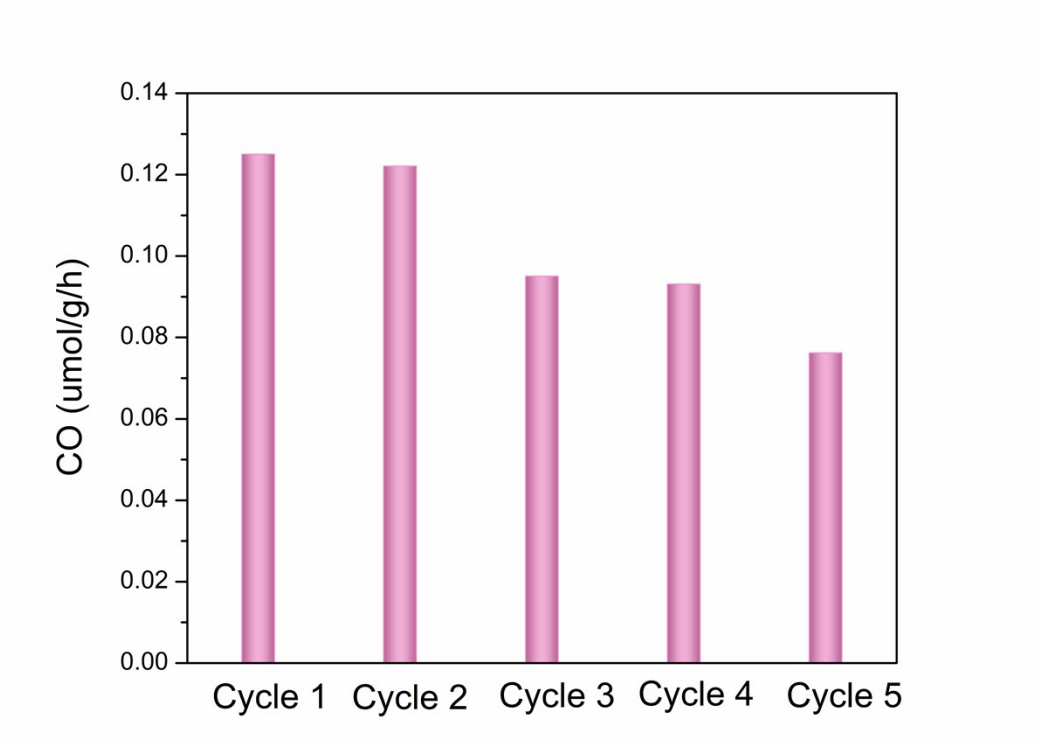

Fig. S5 Cycle experiments of photocatalytic reduction of CO_2 over 100Cu_2O-0.1Pd

Fig. S6 the reaction pressure in actual experiment.

Based on the previous reports [6-7], the poison effect of CO might cause 90% performance decline in catalytic reaction within 0.5 h, namely the catalyst is basically deactivated. However, in our work, a relative stable photocatalytic performance is observed, where the yield of CO demonstrates only 2% decrease (Fig. S5) after first cycle (4 h reaction time). This performance decline is likely attributed to the mass loss of catalyst [8]. Therefore, it should be speculated that no distinct poison effect of CO exists in our system. Here, two aspects are provided as probable explanations. The first should be the negative pressure reaction condition. The whole photocatalytic reaction was performed under -0.04 MPa pressure of CO_2 atmosphere, which is beneficial for the products escaping from the aqueous solution and entering into the online GC detection (Fig. S6). Thus, the generated CO can be promptly extracted from the surface of catalyst in aqueous solution avoiding its poison effect. The second should be the active site location. Since Cu_2O is a p-type semiconductor, according to the energy band matching between 100Cu_2O and Pd, the photoholes as major charge carrier migrate from the valence band of 100Cu_2O to Pd leaving photoelectrons for CO_2 reduction on the surface of 100Cu_2O. Thus, the active site is located on the surface of Cu_2O rather than Pd, which further inhibits the poison effect for Pd by CO.

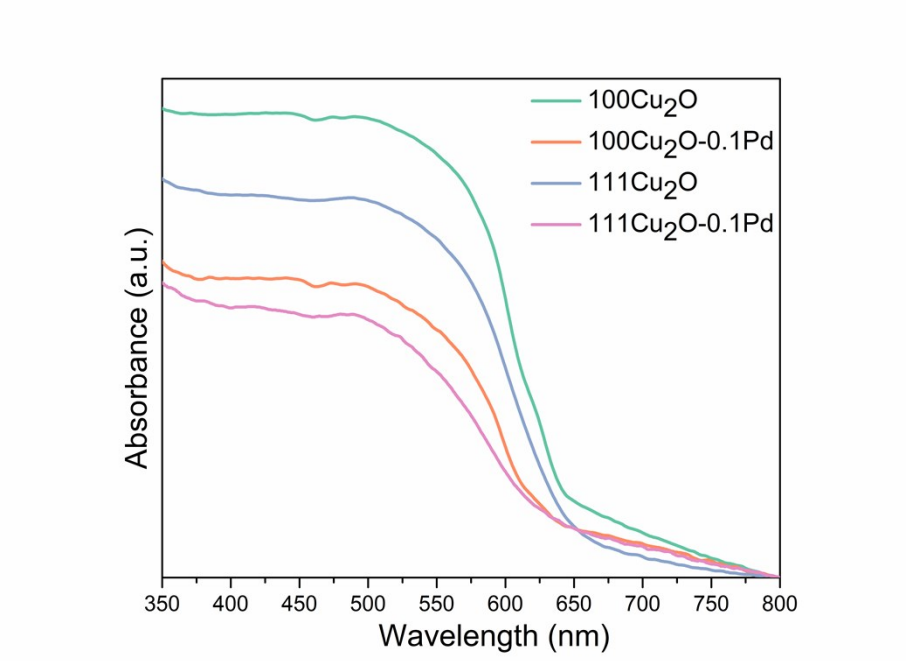

Fig. S7 UV-Vis diffuse reflectance spectra of $100Cu_2O$, $111Cu_2O$, $100Cu_2O$-0.1Pd and $111Cu_2O$-0.1Pd.

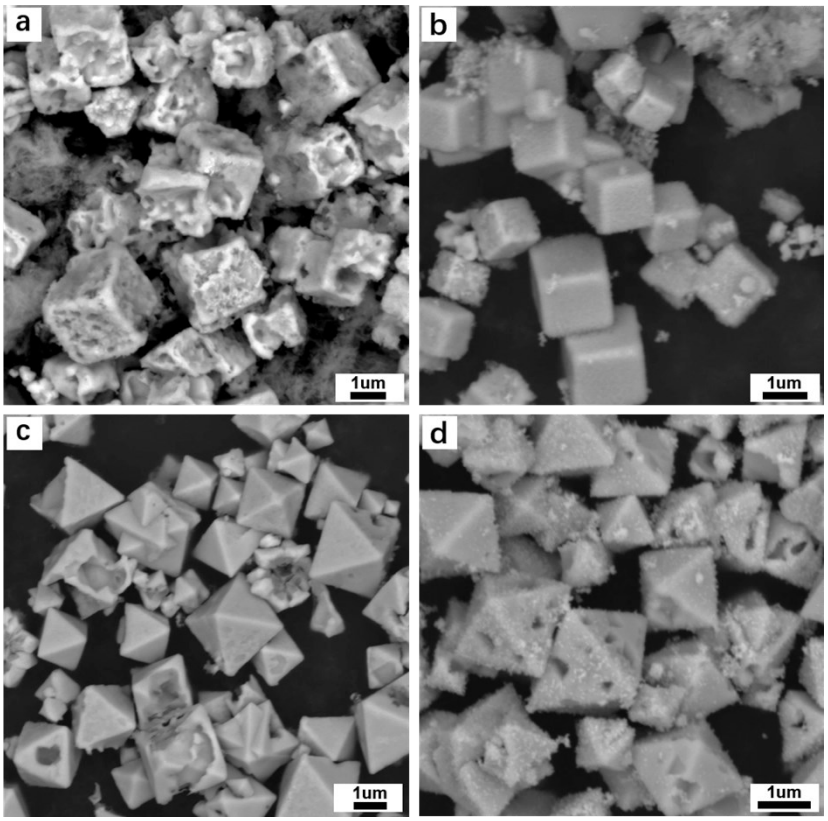

Fig. S8 SEM images of (a) $100Cu_2O$, (b) $100Cu_2O$-0.1Pd, (c) $111Cu_2O$ and (d) $111Cu_2O$-0.1Pd after photoreduction of CO_2.

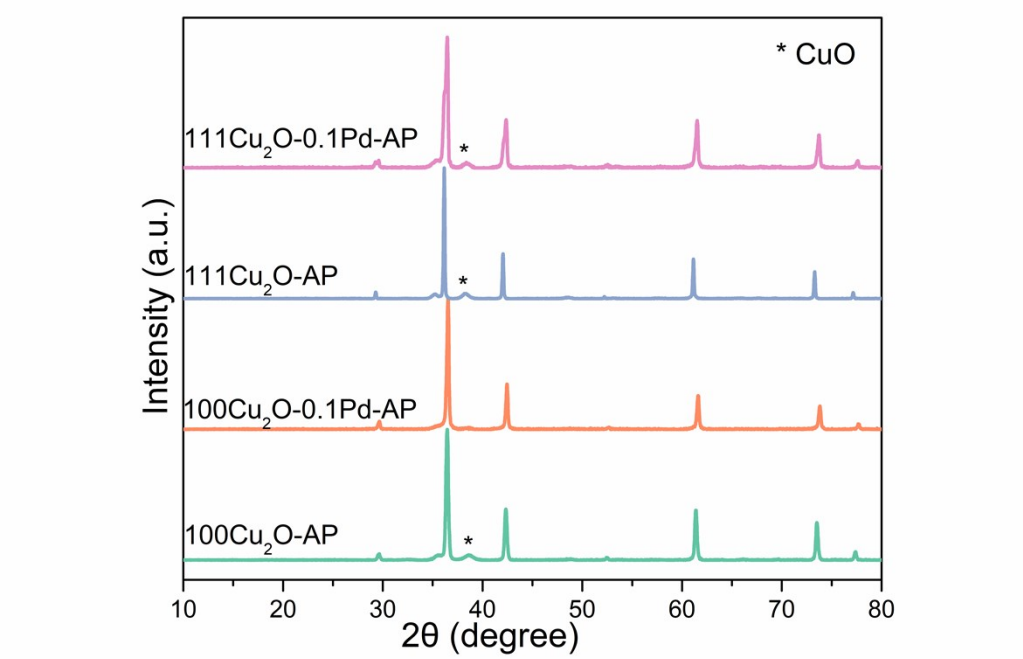

Fig. S9 XRD patterns of $100Cu_2O$, $111Cu_2O$, $100Cu_2O$-0.1Pd and $111Cu_2O$-0.1Pd after photoreduction of CO_2.

TableS1. The binding energy of Cu 2p, O 1s, Pd 3d from XPS spectrum over $100Cu_2O$, $111Cu_2O$, $100Cu_2O$-0.1Pd and $111Cu_2O$-0.1Pd

Samples	Binding Energy (eV)					
	Cu 2p		O 1s		Pd 3d	
	Cu^+	Cu^{2+}	Lattice O	Absorbed O	Pd^0	Pd^{2+}
$100Cu_2O$	931.9; 951.8	933.4; 953.4 942.5; 962.1	529.8	531.1		
$100Cu_2O$-0.1Pd	931.8; 951.7	933.7; 953.6 941.3;961.8; 943.7	529.3	530.8 533.0	335.0; 340.3	336.1; 341.4
$111Cu_2O$	931.6; 951.5	933.4; 953.4 942.6; 962.1	529.6	530.5		
$111Cu_2O$-0.1Pd	931.6; 951.4	933.5;953.3 941.8; 961.8	529.7	530.8 532.1	334.8; 340.1	336.7; 342.2

Table.S2 The Multi-point BET and CO_2 adsorption of $100Cu_2O$, $111Cu_2O$, $100Cu_2O$-0.1Pd and $111Cu_2O$-0.1Pd

Sample	SBET (m^2g^{-1})	CO_2 adsorption (cc/g)
$100Cu_2O$	3.84	0.255
$100Cu_2O$-0.1Pd	362.88	18.843
$111Cu_2O$	2.22	1.955
$111Cu_2O$-0.1Pd	461.66	25.641

References

[1] Cendula, P.; Tilley, S. D.; Gimenez, S.; Bisquert, J.; Schmid, M.; Grätzel, M.; Schumacher, J. O., Calculation of energy band diagram of a photoelectrochemical water splitting cell. J. Phys. Chem. C., 2014, 118, 51, 29599–29607.

[2] Chu, C. Y.; Huang, M. H., Facet-dependent photocatalytic properties of Cu_2O crystals probed by using electron, hole and radical scavengers. J. Mater. Chem. A, 2017, 5, 15116–15123

[3] Balamurugan, B.; Aruna, I.; Mehta, B. R., Size-dependent conductivity-type inversion in Cu_2O nanoparticles. Phys. Rev. B., 2004, 69, 165419-165424.

[4] Tan, C. S.; Hsu, S. C.; Ke, W. H.; Chen, L. J.; Huang, M. H., Facet-dependent electrical conductivity properties of Cu_2O crystals. Nano. Lett., 2015, 15, 2155-2160.

[5] Maeda, K., Metal-complex/semiconductor hybrid photocatalysts and photoelectrodes for co2 reduction driven by visible light. Adv. Mater., 2019, 31, 1808205-1808242.

[6] Min, X. Q.; Kanan, M. W., Pd-catalyzed electrohydrogenation of carbon dioxide to formate: high mass activity at low overpotential and identification of the deactivation pathway. J. Am. Chem. Soc,. 2015, 137, 4701-4708.

[7] Wang, J. Y.; Zhang, H. X.; Jiang, K.; Cai, W. B., From HCOOH to CO at Pd electrodes: a surface-enhanced infrared spectroscopy study. J. Am. Chem. Soc., 2011, 133, 14876-14879.

[8] Aguirre, M. E.; Zhou, R.; Eugene, A. J.; Guzma, M. I.; Grela, M. A., Cu_2O/TiO_2 heterostructures for CO_2 reduction through a direct Z-scheme: Protecting Cu_2O from photocorrosion. Appl. Catal. B, 2017, 217, 485-493.